Published in final edited form as:
Eur J Immunol. 2013 May ; 43(5): 1195–1207. doi:10.1002/eji.201242881.

Diversification and senescence of Foxp3+ regulatory T cells during experimental autoimmune encephalomyelitis

Sharyn Tauro[*], **Phuong Nguyen**[*], **Bofeng Li**[*], and **Terrence L. Geiger**[*]
[*]Department of Pathology, St. Jude Children's Research Hospital, Memphis, TN, USA 38120

Abstract

The fate of Foxp3$^+$ regulatory T cells (Treg) responding during autoimmunity is not well defined. We observed a marked elevation in KLRG1$^+$ CNS-infiltrating Treg in experimental autoimmune encephalomyelitis (EAE), and assessed their origin and properties. KLRG1$^+$ Treg showed increased activation marker expression, Foxp3 and CD25 levels, and more rapid cell cycling than KLRG1$^-$ cells. KLRG1$^-$ Treg converted into KLRG1$^+$ cells and this was increased in the context of autoimmune inflammation. Conversion was unidirectional; KLRG1$^+$ Treg did not revert to a KLRG1$^-$ state. KLRG1$^+$ but not KLRG1$^-$ Treg survived poorly, indicative of terminal differentiation. This was associated with diminished BCL2 and increased apoptosis of isolated cells. KLRG1 was not upregulated on iTreg in culture, but was after transfer and EAE induction or on iTreg developing spontaneously during EAE. KLRG1$^+$ Treg produced more IL10 and had altered effector cytokine production compared with KLRG1$^-$ Treg. Despite their differences, KLRG1$^+$ and KLRG1$^-$ Treg proved similarly potent in suppressing EAE. KLRG1$^+$ and KLRG1$^-$ populations were phenotypically heterogeneous, with the extent and pattern of activation marker expression dependent both on cellular location and inflammation. Our results support an extensive diversification of Treg during EAE, and associate KLRG1 with altered Treg function and senescence during autoimmunity.

Keywords

Regulatory T cell; Foxp3; KLRG1; T cell senescence; EAE; autoimmunity

Introduction

Foxp3 expression identifies an essential population of immunoregulatory CD4$^+$ T lymphocytes that restrain autoimmune and inflammatory responses[1–3]. Foxp3 deficiency leads to fulminant multi-organ autoimmunity. CD4$^+$Foxp3$^+$ T cells (Treg) are stimulated in an antigen-specific manner, and may suppress target cells either directly or by locally modulating the cellular milieu.

In experimental allergic encephalomyelitis (EAE), an animal model of Multiple Sclerosis, Treg rapidly expand in the inflamed CNS[4]. As the disease peaks and then regresses the proportion of CNS-infiltrating Treg increases, often reaching 20–40% of total CD4$^+$ T cells[5]. Depletion of Treg exacerbates EAE immunopathology, whereas supplementation through adoptive immunotherapy is protective[6–9].

Address correspondence to: Terrence L. Geiger, M.D., Ph.D. Member, Department of Pathology, St. Jude Children's Research Hospital, 262 Danny Thomas Pl., MS 342, Memphis, TN 38105, terrence.geiger@stjude.org.

KLRG1 is a low affinity, ITIM-bearing receptor for cadherin-family proteins[10]. It is expressed on NK cells and a minority of CD4 and CD8 T cells. KLRG1 has been more thoroughly studied on CD8 than CD4 T cells, though on both cell types is associated with T cell activation and senescence[11–15]. Terminally differentiated effector T cells express high levels of KLRG1, while long-lived memory cells express low levels. Though KLRG1 serves as a marker for senescence, signaling through KLRG1 has not been causally associated with this. Indeed, KLRG1$^{-/-}$ mice demonstrate unaltered T cell function[16] and a recent study associated KLRG1 with initial priming conditions rather than ultimate cell fate[17].

In addition to Foxp3^{-} T cells, KLRG1 is also expressed on a small population of Foxp3^{+} Treg[18;19]. One recent study identified increased KLRG1 expression among Treg that displayed properties of memory T cells, though whether the memory population was confined to the KLRG1^{+} subset was not determined[20]. Analysis of KLRG1^{+} Treg indicated that they are somewhat more potent than KLRG1^{-} cells in suppressing naïve T cell proliferation *in vitro*, but display other properties characteristic of Treg, including diversity in TCR usage and decreased responsiveness to TCR stimulation[18]. KLRG1^{+} cells were increased among Treg in draining lymph nodes after s.c. LPS injection, indicating that they are induced or selectively recruited with inflammation, and increased KLRG1 message was identified in Treg during chronic helminth infection[19;21]. KLRG1 was also upregulated on CD4^{+}Foxp3^{-} T cells that convert into Foxp3^{+} Treg after transfer into lymphopenic Rag$^{-/-}$ hosts[22]. These data associate KLRG1 expression on Treg with activating conditions.

To better establish the origin and function of KLRG1^{+} Treg in the context of autoimmunity, we examined this population in mice with EAE. We demonstrate that KLRG1^{+} Treg comprise a functionally distinct Treg maturation subset. They show rapid proliferation, an altered cytokine production profile, and limited *in vivo* survival, though are as potent as KLRG1^{-} Treg in suppressing disease. We further demonstrate that KLRG1 can be upregulated during EAE independently of other markers associated with Treg activation, including CD103, PD-1, and LAG3. Our results are consistent with a broad phenotypic diversification of Treg responding during autoimmunity, and indicate that KLRG1 identifies a functionally active though senescent Treg population.

Results

Expansion and localization of KLRG1^{+} Treg during EAE

KLRG1 is only expressed on a minority of Treg. Fewer than 1% and 4% of CD4^{+}CD8^{-}Foxp3^{+} thymocytes in mice ≤4 and 52 wk old respectively expressed KLRG1 (Fig. 1a). KLRG1 was expressed on a larger though still small proportion of Treg in the spleen, ~4% of cells at 1 wk increasing to ~6–10% in older mice.

After the induction of EAE with myelin oligodendrocyte glycoprotein $(MOG)_{35–55,}$ the proportion of Treg expressing KLRG1 increased on average 4.4 fold and 3.2 fold respectively in the draining (inguinal) lymph nodes (DLN) and spleen (Fig. 1b). KLRG1^{+} Treg were more dramatically increased in the CNS, comprising >38% of Foxp3^{+} cells. Because Treg expand more rapidly than conventional CD4^{+} T cells during EAE, KLRG1^{+} Treg showed an even greater fractional rise as a proportion of the total CD4^{+} T cell population that they regulate than as a proportion of Treg (Fig. 1c). KLRG1 expression among CNS Treg was positively correlated with disease severity, increasing from 23.4±5.3% to 47.5±3.3% as disease score advanced from 1 to 4 ($p<0.001$) (Fig. 1d).

The fraction of KLRG1$^+$ cells was substantially greater among CD4$^+$Foxp3$^+$ than Foxp3$^-$ T cells. Fewer than 1% of CD4$^+$Foxp3$^-$ T cells expressed KLRG1 in the thymus, spleens, and LN of mice without disease (Suppl. Fig. 1a and not shown). In mice with EAE, the proportion of non-Treg expressing KLRG1 was on average 7.1, 9.2, and 2.9-fold lower than that of Treg in the DLN, spleen, and CNS respectively. Further, the mean fluorescence intensity (MFI) of KLRG1 stained on KLRG1$^+$Foxp3$^-$ cells was ~1log10 less than on KLRG1$^+$Foxp3$^+$ cells (Suppl. Fig. 1b, c). Therefore, KLRG1 expression is markedly and selectively increased among Treg during EAE.

KLRG1$^+$ Treg in EAE are Foxp3^{hi}, CD25^{hi}, and demonstrate an activated phenotype

Treg have been divided into functionally distinct subsets based on Foxp3 and CD25 expression, and loss of Foxp3 may be associated with degeneration into effector populations[23–28]. Foxp3 and CD25 expression was, however, stable or modestly increased on KLRG1$^+$ compared with KLRG1$^-$ Treg from the spleen or LN of mice with or without EAE, indicating retention of a regulatory phenotype (Fig. 2). CD25 was more markedly elevated on CNS Treg of diseased mice. KLRG1$^+$ Treg also showed decreased expression of CD62L, and increased CD44, Helios, and GITR compared with paired KLRG1$^-$ Treg from the same mice and organs (Fig. 2). Therefore KLRG1 is associated with an activated Treg phenotype[29;30]. However, KLRG1 is not obligately induced on activated Treg, as decreased CD62L and increased CD44, Helios, GITR, and CD25 was also seen on KLRG1$^-$ Treg from mice with EAE compared with control mice, though to a lesser extent.

KLRG1 upregulation on iTreg during EAE

We previously showed that there is little induced Treg (iTreg) formation during MOG-EAE, indicating that the KLRG1 upregulation we observed is occurring on natural Treg[31;32]. To determine whether iTreg also express KLRG1, we generated these by stimulating CD4$^+$Foxp3$^-$ T cells in the presence of IL-2 and TGF-β. KLRG1 was not expressed by the iTreg or residual Foxp3$^-$ cells in the cultures (Fig. 3a). Sorted CD4$^+$Foxp3$^+$ iTreg transferred into either Rag1$^{-/-}$ or lymphoreplete CD45-congenic recipients similarly failed to upregulate KLRG1 (Fig. 3b, c, e and Suppl. Fig. 2a). Consistent with our and others' reports, the transferred iTreg poorly retained Foxp3 [33;34]. KLRG1 was also not detected on these Foxp3$^-$ revertants.

To determine if iTreg would upregulate KLRG1 in the context of EAE, we transferred Foxp3$^+$ cells to lymphoreplete mice prior to EAE induction. Seven days after immunization, KLRG1 was readily detected on a subset of iTreg (Fig. 3d, e). iTreg may also form from conventional T cells *in vivo*, though phenotypic markers definitively distinguishing them from nTreg are lacking. To examine such iTreg, we bred MOG-specific 2D2 TCR Tg mice onto a Rag1$^{-/-}$ background. These mice lack Foxp3$^+$ Treg due to their monoclonal TCR. After disease induction, Foxp3 was upregulated on a small fraction of CNS T cells (<1%), indicative of iTreg formation (Fig. 3f). A subset of these expressed KLRG1. A small proportion of 2D2/Rag1$^{-/-}$ mice additionally develop spontaneous EAE (<5%). iTreg formed in these mice too, and a subset also upregulated KLRG1 (Fig. 3g). Therefore, KLRG1 can be induced on iTreg, and this requires an inflammatory context that may be provided by induced or spontaneous autoimmunity.

Increased in situ proliferation of KLRG1$^+$ Treg

Considering the limited iTreg formation during MOG-EAE[31], the increase in KLRG1$^+$ Treg number could not be explained by Foxp3 induction on KLRG1$^+$ Foxp3$^-$ T cells. This population's expansion may have been due to KLRG1 induction on KLRG1$^-$ Treg, or decreased death or increased expansion rates of pre-existing KLRG1$^+$ cells.

To assess the cell cycle rate among the different populations, we pulsed unimmunized controls or mice with EAE with BrdU for 16 h, and measured the nucleotide analog's incorporation into KLRG1$^+$ or KLRG1$^-$ Treg. Splenic and LN Treg from mice with EAE, whether KLRG1$^+$ or KLRG1$^-$, showed significantly increased BrdU uptake compared with control mice. However, KLRG1$^+$ Treg also showed significantly more BrdU incorporation than paired KLRG1$^-$ Treg populations from the same mice and organs, indicating an increased expansion rate (Fig. 4a, b). We confirmed this finding by staining for Ki67, a marker excluded from resting (G0) cells (Fig. 4c, d). Therefore, KLRG1 positivity is associated with increased cell cycling *in situ* regardless of the presence of disease, though the proliferation rate is globally augmented in Treg during autoimmune inflammation.

KLRG1 is unidirectionally induced on KLRG1$^-$ Treg and marks a senescent population

As an additional explanation for the increased representation of KLRG1$^+$ Treg in EAE, we examined the stability and interconversion of the KLRG1$^+$ and KLRG1$^-$ populations. KLRG1$^+$ and KLRG1$^-$ Treg were flow cytometrically purified from GFP-Foxp3 donor mice with or without EAE, and equal quantities transferred into Rag1$^{-/-}$ recipients. Alternatively, in competition experiments, CD45 congenic KLRG1$^+$ and KLRG1$^-$ Treg isolated from mice with EAE were co-transferred into Rag1$^{-/-}$ hosts. Seven days after transfer, the cells were analyzed. For both experimental formats, Foxp3 expression was stable in both the KLRG1$^+$ and KLRG1$^-$ populations. A population of CD4$^+$TCR$^+$ cells downmodulating Foxp3 could not be resolved (Fig. 5a, left panel, Suppl. Fig. 2b, and not shown).

Virtually all transferred KLRG1$^+$ cells retained KLRG1 expression at d 7 after transfer, regardless of whether they were co-transferred with KLRG1$^-$ cells and whether they were derived from mice with EAE (Fig. 5a, b, d). In contrast, transferred KLRG1$^-$ Treg did not remain KLRG1$^-$. They upregulated KLRG1 in association with homeostatic expansion in the lymphopenic hosts. This result differed from that obtained with iTreg, which remained uniformly KLRG1$^-$ after transfer into lymphopenic recipients (Fig. 3b, e). The extent of KLRG1 upregulation was independent of whether the KLRG1$^-$ cells were co-transferred with KLRG1$^+$ cells, indicating that the presence of KLRG1$^+$ Treg does not alter the conversion rate. However, more KLRG1$^-$ Treg from mice with EAE than from control unimmunized mice upregulated KLRG1 (Fig. 5c, 49.4±7.3% and 26.0±7.9% for KLRG1$^-$ transfer from mice with or without EAE; Fig. 5d, 50.3±4.4% for transferred KLRG1$^-$ cells from mice with EAE co-transferred with KLRG1$^+$ cells). Therefore, KLRG1$^-$ Treg unidirectionally mature into KLRG1$^+$ progeny. The magnitude of this is influenced by the cells' prior exposure to inflammatory stimuli.

In experiments where KLRG1$^+$ and KLRG1$^-$ Treg were co-transferred, it was also possible to assess the relative fitness of the two populations. Approximately equal numbers of KLRG1$^+$ and KLRG1$^-$ Treg were co-transferred into the Rag1$^{-/-}$ mice. However, at the end of 7 days, cells derived from the transferred KLRG1$^-$ Treg outcompete the transferred congenic KLRG1$^+$ cells, indicating an increased fitness of the KLRG1$^-$ population (Fig. 5e).

To better define the relationship between the Treg subsets we also performed transfers into lymphoreplete mice. We co-transferred CD45-congenic Thy1.2$^+$ KLRG1$^+$ and KLRG1$^-$ Treg isolated from mice with EAE into Thy1.1$^+$ C57BL/6 recipients. Alternatively, CD45.2$^+$ KLRG1$^+$ or KLRG1$^-$ Treg were independently transferred into CD45.1 congenic mice. EAE was induced 1 d after transfer and mice were analyzed 7 d later. Although equivalent numbers of KLRG1$^+$ and KLRG1$^-$ Treg were transferred, 7 d after EAE induction, few of the transferred KLRG1$^+$ cells were detected in either the DLN or spleen (Suppl. Table I and Suppl. Fig. 3). Indeed, in 3 of 4 mice receiving co-transferred KLRG1$^+$ and KLRG1$^-$ Treg, no KLRG1$^+$ cells were identified in the spleen. In the DLN, the mean ratio of Treg derived from co-transferred KLRG1$^-$ to KLRG1$^+$ cells was >2log10 (range

15.8 – 363.5). Although small numbers of the transferred KLRG1$^-$ Treg were found in the lung and liver, the transferred KLRG1$^+$ cells were not detected there or in the CNS, indicating that the loss of the KLRG1$^+$ Treg did not result from altered migration to these locations (not shown). Therefore KLRG1$^+$ Treg survive poorly *in vivo*. The transferred KLRG1$^-$ Treg were better maintained. As with transfers into Rag1$^{-/-}$ mice, a significant fraction upregulated KLRG1 (Suppl. Table I and Suppl. Fig. 3).

Increased cell death among KLRG1$^+$ Treg

The senescent state of transferred KLRG1$^+$ Treg implied an increased cell death rate. To further assess this, we examined directly isolated cell populations for phosphatidylserine inversion and membrane permeability by Annexin V (AnnV) and propidium iodide (PI) staining (Fig. 6a, b). KLRG1$^+$ Treg from the LN, spleen, and CNS of mice with or without EAE showed substantially increased proportions of total non-viable (AnnV$^+$ and/or PI$^+$), late apoptotic (AnnV$^+$PI$^+$), and dead (AnnV$^-$PI$^+$) cells compared with the KLRG1$^-$ Treg in the same samples. An increase in early apoptotic cells (AnnV$^+$PI$^-$) was also observed in the spleen and DLN of mice with EAE, and spleen of control mice, and a non-significant trend was observed in control LN and CNS of mice with EAE. This indicates an increased apoptotic susceptibility of KLRG1$^+$ compared with KLRG1$^-$ Treg.

Cells were additionally stained for the antiapoptic protein BCL2, as well as FAS and FASL (Suppl. Fig. 4). BCL2 levels were diminished in KLRG1$^+$ compared with the KLRG1$^-$ Treg from all sites tested, consistent with the diminished KLRG1$^+$ Treg survival. FAS levels were modestly diminished on the KLRG1$^-$ Treg from all sites except the CNS. However, susceptibility to FAS induced death is increased with T cell activation, and the functional significance of this finding is uncertain. Accompanying the enhanced expression of other activation markers, FASL levels were also increased in KLRG1$^+$ Treg, suggesting that these cells also have a greater potential to mediate cell death through the FAS pathway.

Distinct cytokine profiles of KLRG1$^+$ and KLRG1$^-$ Treg

Treg demonstrate variable cytokine production profiles. A subset of Treg express IL10, which we and others have previously demonstrated to be important for EAE suppression[6;8;35]. Other Treg express effector cytokines, including IFNγ and IL17, which have not been evaluated in EAE for Treg-specific impact[1]. We used intracellular staining (ICS) to compare IL10, IL17 and IFNγ production by KLRG1$^+$ and KLRG1$^-$ Treg from the LN, spleen, and CNS of mice with EAE or controls.

KLRG1$^+$ and KLRG1$^-$ Treg demonstrated different cytokine profiles. IL10 expression was elevated among KLRG1$^+$ Treg (Fig. 7a, b). This proved significant among the DLN and splenocytes of mice with EAE. A trend toward increased IL10 was also seen among CNS-infiltrating Treg ($p=0.09$). This implies that KLRG1$^+$ Treg are an important source of Treg-derived IL10. IFNγ production showed a similar pattern, with KLRG1$^+$ cells showing elevated production compared with KLRG1$^-$ cells, and this proved significant in all tissues from mice with EAE. The role of IFNγ in EAE is not fully established. IFNγ$^{-/-}$ mice develop more severe EAE than wild type controls, and the timing and location of IFNγ expression appears important in determining its role[36;37]. In contrast, IL17 expression was uniformly diminished in the KLRG1$^+$ population. These cytokine expression patterns were paralleled in analyses of gene expression by qRT-PCR, with sorted splenic KLRG1$^+$ Treg demonstrating increased IL10 and IFNγ, and diminished IL17 relative to KLRG1$^-$ cells (Fig. 7c). Therefore KLRG1$^+$ and KLRG1$^-$ Treg in mice with EAE possess distinct functional capacities.

KLRG1$^+$ and KLRG1$^-$ Treg are similarly potent inhibitors of EAE

In a prior study, KLRG1$^+$ Treg demonstrated increased *in vitro* potency when compared with KLRG1$^-$ cells in suppressing naïve T cell proliferation [18]. CNS-infiltrating Treg have been shown to suppress EAE development after adoptive transfer[38]. To test the relative potency of CNS-infiltrating KLRG1$^+$ and KLRG1$^-$ Treg populations *in vivo*, we flow cytometrically isolated them from diseased GFP-Foxp3 mice. 5×10^4 cells were then transferred into recipients prior to disease induction. Mice treated with saline, or with a 20-fold greater number (10^6) of culture-derived iTreg were compared as controls. Both KLRG1$^+$ and KLRG1$^-$ Treg efficiently suppressed EAE (Fig. 8 and Suppl. Table II). In one of two experiments, the KLRG1$^+$ Treg showed greater potency than KLRG1$^-$ Treg as determined by integrated disease score (AUC analysis, Suppl. Table II). However, this increase was modest. Therefore, KLRG1$^+$ and KLRG1$^-$ Treg demonstrate similar disease suppressive capacities despite the decreased lifespan of the KLRG1$^+$ cells.

Phenotypic diversification of the Treg response during EAE

We next examined the phenotypic diversity of the KLRG1$^+$ Treg subset. CD103, PD-1, and LAG3 bear binary expression patterns on Treg and have been associated with Treg functional capacity[39–41]. We examined co-expression of these individual markers on Treg from the LN, spleen, and CNS from mice with or without EAE (Fig. 9 and Suppl. Fig. 5). Varying patterns of co-expression with KLRG1 were seen. KLRG1$^+$ Treg expressed high and fairly consistent levels of PD-1 in organs from unimmunized controls and mice with EAE whereas elevated expression of PD-1 was only seen among KLRG1$^-$ Treg in the CNS of mice with EAE (Fig. 9a). CD103 co-expression with KLRG1 was common on Treg from non-immune LN, 89±1%, though less frequent in other groups or among KLRG1$^-$ Treg. In contrast, LAG3 expression was most commonly seen on CNS-infiltrating KLRG1$^+$ Treg, 55±9%. Increased LAG3 expression was also seen in KLRG1$^-$ Treg in the CNS, but to a lower extent. Therefore each marker demonstrates variability in expression that is dependent on location and disease status. Though in any individual location PD-1, CD103, and LAG3 are more often expressed on KLRG1$^+$ than KLRG1$^-$ Treg, expression is not obligately linked to KLRG1 per se.

Correlation of the co-expression of all 4 markers showed that the majority of Treg in control mice were negative for KLRG1, CD103, PD-1, and LAG3 (Fig. 9b). In the spleen and LN of mice with EAE, an increased percent of Treg expressed at least one marker, though differences from unimmunized mice were modest. More notably, <15% of CNS Treg were negative for all markers, and nearly 60% were positive for 2 or more markers. Specific co-expression patterns were apparent among the markers and these were dependent on both location and disease status (Fig. 9c). For example, in the CNS, PD-1 was most commonly present when only a single additional marker was expressed on either the KLRG1$^+$ or KLRG1$^-$ Treg subsets. When a second additional marker was expressed, LAG3 was more commonly associated with PD-1 than CD103 for both the KLRG1$^+$ and KLRG1$^-$ populations. Co-expression of LAG3 and CD103 in the absence of PD-1 was uncommon. These data are consistent with an extensive and context-dependent phenotypic diversification of the Treg during EAE, and indicate that KLRG1$^+$ and KLRG1$^-$ Treg may be further dissected into phenotypically discrete subpopulations.

Discussion

During EAE, Treg infiltrate the CNS where they rapidly expand and limit autoinflammatory damage[5;42]. As a prelude to these studies, we explored differences in CNS-infiltrating or non-infiltrating Treg using expression arrays and flow cytometry. This prompted us to further evaluate Treg expression of KLRG1.

We demonstrate an increase in KLRG1 expression among Treg in mice with EAE, particularly in the CNS. The prevalence of KLRG1$^+$ Treg in the CNS positively correlated with disease severity, associating these cells with the response to tissue inflammation. KLRG1$^+$ Treg showed a predominantly memory/activated phenotype as determined by CD44, CD62L, Helios, and GITR expression, whereas KLRG1$^-$ Treg demonstrated more variability in this regards. KLRG1$^+$ Treg were also uniformly CD25^{hi} and Foxp3^{hi}, indicating that they maintain a regulatory phenotype. Indeed, CD25 was prominently upregulated on CNS-infiltrating KLRG1$^+$ Treg. However, CD25 and other activation markers were also increased on KLRG1$^-$ cells, indicating that both subsets are activated during EAE, and that KLRG1 upregulation is not a necessary outcome of Treg activation in the CNS.

nTreg dominate the Treg response in mice with EAE[31;32], though smaller numbers of iTreg are identifiable. TCR Tg/Rag$^{-/-}$ mice fail to develop nTreg, though under specific conditions, such as with provision of low dose or oral Ag, iTreg may form[43;44]. Using MOG-specific TCR Tg/Rag$^{-/-}$ mice, we could visualize iTreg induction during both induced and spontaneous EAE. A proportion of these upregulated KLRG1, indicating that in an appropriate environment both nTreg and iTreg can express KLRG1. Considering the clonality of these TCR Tg/Rag$^{-/-}$ cells, it would seem that specificity does not alone dictate KLRG1 expression. However, further studies will be needed to determine whether and how TCR specificity impacts Treg cell fate decisions.

We further mapped the fate and origin of KLRG1$^+$ and KLRG1$^-$ Treg. Both BrdU incorporation and Ki67 staining indicated an increased rate of cell cycling among KLRG1$^+$ cells, regardless of the presence of EAE, though it is not possible to establish whether the KLRG1$^+$ population is homogeneous in this regards or contains subsets with variable proliferation rates. In one study, conventional CD8 T cells expressing KLRG1 displayed a modestly increased fraction in cell cycle, suggesting that the cellular program inducing KLRG1 on Treg may have some commonalities with that in other T cell types[45]. EAE further enhanced the proliferation rate above that seen in unmanipulated mice, though this was observed for both KLRG1$^+$ and KLRG1$^-$ Treg. Indeed, there was a greater fold increase in the proliferation rate of KLRG1$^-$ than KLRG1$^+$ Treg in either the LN or spleen from mice with EAE when compared with unimmunized mice. Therefore, though KLRG1$^+$ Treg appear to be overall proliferating more rapidly than KLRG1$^-$ Treg, it would seem unlikely that this alone is responsible for their increased representation in mice with EAE.

Fate mapping studies provided an alternative explanation for the increased prevalence of KLRG1$^+$ Treg during EAE. These demonstrated a unidirectional conversion of KLRG1$^-$ into KLRG1$^+$ Treg. We found few KLRG1$^+$ Treg in the thymus, suggesting that the larger peripheral population of KLRG1$^+$ Treg is formed extrathymically. This was directly apparent in transfers into either lymphopenic or lymphoreplete mice.

Though KLRG1 was upregulated on both iTreg and nTreg in the setting of EAE, only nTreg upregulated KLRG1 after transfer into lymphopenic recipients. We are currently uncertain of the significance of this discrepancy, but suspect that the different cellular programming of culture-derived iTreg and nTreg influences KLRG1 expression in lymphopenic conditions. In a similar regard, it is interesting that KLRG1 has been identified on a subset of iTreg that forms *in vivo* after CD4$^+$Foxp3$^-$ T cell transfer into lymphopenic hosts[22]. This indicates that KLRG1$^+$ iTreg can form with homeostatic proliferation, though it is possible that after CD4$^+$Foxp3$^-$ T cell transfer KLRG1 is upregulated on conventional T cells prior to Foxp3 upregulation rather than on the Foxp3$^+$ iTreg themselves. iTreg used in our transfers were formed *in vitro* through stimulation with IL-2, TGF-β, and TCR agonists and not *in vivo*. It

is thus also possible that the different types of iTreg have distinct programming and potential to mature into the KLRG1$^+$ subset.

KLRG1$^+$ Treg had a brief lifespan, with few remaining 1 wk after transfer to C57BL/6 mice. In the context of lymphopenia, the loss of KLRG1$^+$ T cells was less substantial, implying that homeostatic signals there help maintain the KLRG1$^+$ population. Identifying signaling pathways preserving KLRG1$^+$ Treg will be important, and may identify approaches to support these cells during immunopathologic conditions.

As this manuscript was being finalized, Cheng and colleagues similarly reported that KLRG1$^-$ Treg, transferred into lymphopenic mice in conjunction with non-regulatory T cells, can upregulate KLRG1 and that transferred KLRG1$^+$ cells demonstrate a diminished lifespan[46]. Our analyses in the context of autoimmunity are fully consistent with these findings, which cumulatively indicate that KLRG1 is induced on Treg in the setting of EAE, and that these KLRG1$^+$ cells are destined to die. Notably, in non-regulatory T cells, KLRG1 is a marker for cell fate but not responsible for this fate, and studies of KLRG1-deficient mice will be important to further evaluate KLRG1's impact on Treg.

Although relatively few Treg can be identified that produce cytokines *in situ*, IL10 is particularly important for Treg function, and we and others have shown that Treg-produced IL10 is a critical regulator of EAE severity[6;8]. KLRG1$^+$ Treg demonstrated enhanced IL10 production when compared with KLRG1$^-$ Treg in mice with EAE. IL10 may be expressed by virtually all T cell types, though this is usually a late event and associated with a high level of inflammation. These results may imply that inflammatory signaling during EAE induces Treg to enter a terminally differentiated state where they possess increased regulatory potency. It is however noteworthy that a larger proportion of KLRG1$^+$ than KLRG1$^-$ Treg also express IFNγ, which is often viewed as a pathologic cytokine associated with Th1 development. In EAE, IFNγ has mixed roles, both promoting the Th1 differentiation and inhibiting the autoimmune response[37;47]. The impact of Treg produced IFNγ is uncertain. The decreased percentage of KLRG1$^+$ Treg expressing IL17, which is pro-inflammatory in EAE[48], and their increased expression of Foxp3 would further argue against these Treg being pro-inflammatory or comprising a population de-differentiating into Foxp3$^-$ effectors[1].

Despite their decreased lifespan and altered functional status, KLRG1$^+$ Treg from the CNS are as, or potentially slightly more, effective than KLRG1$^-$ cells in inhibiting EAE. Therefore KLRG1$^+$ Treg do form a bona fide, highly active, though terminal population of suppressive T cells. Considering that within a week few transferred KLRG1$^+$ Treg can be detected in mice immunized to induce EAE in either lymphoid or non-lymphoid organs, it would seem most likely that the KLRG1$^+$ cells are acting at the site of priming and not in the CNS.

The magnitude of the diversification of Treg during autoimmunity has not been resolved. To better understand this, we focused on 3 additional markers, PD-1, LAG3, and CD103, each of which is associated with Treg function, and, like KLRG1, demonstrate a binary expression pattern on Treg. Multi-color flow cytometry of CD4$^+$TCR$^+$Foxp3$^+$ T cells using these markers allowed us to correlate their expression with KLRG1. All 16 of the possible combinations of the 4 markers were detected on Treg, however the size of each population varied. Further, location and environment altered the prominence of individual populations. Not surprisingly, our data identified the greatest level of phenotypic diversity in the CNS of mice with EAE. Overall, these results indicate a phenotypic radiation of Treg during active autoimmunity. Defining the fates and origins, deciphering the functional capacities, and

identifying the environmental cues leading to the formation of these different Treg populations will be important.

Materials and Methods

Mice and EAE induction

C57BL/6J and B6.129S7-*Rag1*$^{tm1Mom/J}$ (Rag1$^{-/-}$) mice were purchased from The Jackson Laboratories. GFP-Foxp3 knock in mice were obtained from Dr. A. Rudensky, and back-crossed onto C57BL/6J or congenic B6.SJL-*Ptprc*^{a} *Pepc*^{b}/BoyJ (CD45.1) and B6.PL-*Thy1*^{a}/CyJ (Thy1.1) strains. 2D2 TCR transgenic (Tg) mice were obtained from Dr. V. Kuchroo and crossed with Rag1$^{-/-}$ and GFP-Foxp3 mice. Animal studies were approved by the St. Jude Institutional Animal Care and Use Committee. EAE was induced with $MOG_{35–55}$ peptide and scored as described[6].

Flow cytometry

CNS, inguinal lymph node (LN) or corresponding draining LN (DLN), and splenic cells were isolated as described[6]. T lymphocytes were purified from the CNS by density gradient centrifugation. Cells were stained using Abs against CD4, TCRβ, KLRG1, CD45Rb, CD44, CD25, CD62L, PD-1, LAG3, CTLA4, GITR, CD45.1, CD45.2, Thy1.1, Thy1.2, BCL2, FAS, and FASL, and AnnexinV and PI, all purchased from eBioscience. CD103 and Helios specific Abs were obtained from BioLegend and Ki67 from BD Biosciences. Intracellular Foxp3 staining was performed using eBioscience anti-Foxp3 Ab and Foxp3 fixation permeabilization kit. Cells were analyzed on a FACSCalibur® (BD Biosciences) using CellQuest® software (BD Biosciences) or on an LSRII® (BD Biosciences) with FlowJo® (Tree Star) software.

Flow cytometric sorting and adoptive transfers

CD4^{+}GFP-Foxp3^{+}KLRG1^{+} or CD4^{+}GFP-Foxp3^{+}KLRG1^{-} cells were sorted from surface stained CNS or splenic T cells from mice with EAE (d 14) to >98% purity using Mo-Flo (Dako) or Reflection (iCyt) cytometers. Cells were counted using a hemocytometer and purity and cell numbers confirmed by analytic cytometry. Cells, resuspended in PBS, were transferred by retro-orbital injection. Transferred cell numbers varied from 5×10^{4} to 1×10^{6}, as indicated in the text.

Intracellular cytokine staining

Cells from unimmunized mice and mice with EAE were cultured with PMA (50 ng/ml) and ionomycin (2.5 μg/ml) for 2 h followed by an additional 2 h incubation in the presence of 10 μg/ml Monensin (eBioscience), stained for surface markers followed by fixation and permeabilization, and staining with anti-IL10, IL17, IFNγ and/or Foxp3 (eBioscience).

BrdU staining

Mice were injected i.p. with 200 μl BrdU (10 mg/ml) in DPBS. After 16 h, lymphocytes were isolated, stained for cell surface markers, fixed and permeabilized with Cytofix/Cytoperm buffer (BD Biosciences), treated with DNase (300 μg/ml) at 37°C for 1 h, and stained with anti–BrdU-APC (3D4, BD Biosciences).

Real-time PCR

Total RNA was isolated from flow sorted KLRG1^{+} or KLRG1^{-} CD4^{+}GFP-Foxp3^{+} splenocytes using the RNeasy® Minikit (QIAGEN), and cDNA synthesized using Superscript III and oligo (dT) primers (Invitrogen). Quantitative PCR was performed with IL10, IL17A, IFNγ and HPRT primers using the Platinum SYBR green qPCR super mix

system (Bio-rad). cDNA samples were assayed in triplicate and gene expression levels normalized to HPRT. Mean relative gene expression was determined and expressed as $2^{-\Delta Ct}$ ($\Delta Ct=Ct_{gene}-Ct_{HPRT}$). Primer sequences were: IL-10 forward (F), GTGAAAATAAGAGCAAGGCAGTG; IL10 reverse (R), ATTCATGGCCTTGTAGACACC; L17A F, GCTCCAGAAGGCCCTCAG, IL17A R, CTTTCCCTCGCATTGACA; IFNγ F, GGATGCATTCATGAGTATTGC; IFNγ R, GCTTCCTGAGGCTGGATTC; HPRT F, GACCGGTCCCGTCATGC; HPRT R, TCATAACCTGGTTCATCATCGC.

iTreg Production

Flow sorted $CD4^+CD8^-$GFP-$Foxp3^-CD45Rb^{high}$ T cells were stimulated for one day with 100 U/ml rhIL-2, and 10 ng/ml TGF-β in anti-CD3/CD28 Ab coated plates. The cells were then transferred to non-coated plates and cultured for 5 days in the presence of cytokine before flow cytometric analysis and/or sorting.

Statistics

Standard deviations or errors and confidence intervals were calculated with Excel® or PRISM® software. Significance between 2 groups was calculated by 2-tailed t-test or Mann Whitney U test. When >2 groups were simultaneously compared, significance was determined by ANOVA using a Bonferroni correction for multiple comparisons. A $p<0.05$ was considered significant. For multiple comparisons, significance is only shown for indicated groups.

Acknowledgments

The authors thank Richard Cross, Grieg Lennon, Stephanie Morgan, and Jim Houston for assistance with flow cytometry and flow cytometric sorting. Supported by the National Institutes of Health Grant R01 AI056153 (to TLG) and the American Lebanese Syrian Associated Charities (ALSAC)/St. Jude Children's Research Hospital (to all authors).

Abbreviations

Foxp3	forkhead box transcription factor P3
Treg	$Foxp3^+$ regulatory T cell
iTreg	induced Treg
nTreg	natural Treg
LN	inguinal lymph nodes
DLN	draining inguinal lymph nodes
MOG	myelin oligodendrocyte glycoprotein

References

1. Geiger TL, Tauro S. Nature and nurture in Foxp3(+) regulatory T cell development, stability, and function. Hum Immunol. 2012; 73:232–239. [PubMed: 22240298]
2. Josefowicz SZ, Lu LF, Rudensky AY. Regulatory T cells: mechanisms of differentiation and function. Annu Rev Immunol. 2012; 30:531–564. [PubMed: 22224781]
3. Miyara M, Gorochov G, Ehrenstein M, Musset L, Sakaguchi S, Amoura Z. Human FoxP3+ regulatory T cells in systemic autoimmune diseases. Autoimmun Rev. 2011; 10:744–755. [PubMed: 21621000]

4. O'connor RA, Malpass KH, Anderton SM. The inflamed central nervous system drives the activation and rapid proliferation of foxp3+ regulatory T cells. J Immunol. 2007; 179:958–966. [PubMed: 17617587]
5. Liu X, Alli R, Steeves M, Nguyen P, Vogel P, Geiger TL. The T cell response to IL-10 alters cellular dynamics and paradoxically promotes central nervous system autoimmunity. J Immunol. 2012; 189:669–678. [PubMed: 22711892]
6. Selvaraj RK, Geiger TL. Mitigation of Experimental Allergic Encephalomyelitis by TGF-{beta} Induced Foxp3+ Regulatory T Lymphocytes through the Induction of Anergy and Infectious Tolerance. J Immunol. 2008; 180:2830–2838. [PubMed: 18292504]
7. Mekala DJ, Alli RS, Geiger TL. IL-10-dependent infectious tolerance after the treatment of experimental allergic encephalomyelitis with redirected CD4+CD25+ T lymphocytes. Proc Natl Acad Sci USA. 2005; 102:11817–11822. [PubMed: 16087867]
8. Zhang X, Koldzic DN, Izikson L, Reddy J, Nazareno RF, Sakaguchi S, Kuchroo VK, Weiner HL. IL-10 is involved in the suppression of experimental autoimmune encephalomyelitis by CD25(+)CD4(+) regulatory T cells. Int Immunol. 2004; 16 :249–256. [PubMed: 14734610]
9. Kohm AP, Carpentier PA, Anger HA, Miller SD. Cutting edge: CD4+CD25+ regulatory T cells suppress antigen-specific autoreactive immune responses and central nervous system inflammation during active experimental autoimmune encephalomyelitis. J Immunol. 2002; 169:4712–4716. [PubMed: 12391178]
10. Li Y, Hofmann M, Wang Q, Teng L, Chlewicki LK, Pircher H, Mariuzza RA. Structure of natural killer cell receptor KLRG1 bound to E-cadherin reveals basis for MHC-independent missing self recognition. Immunity. 2009; 31:35–46. [PubMed: 19604491]
11. Reiley WW, Shafiani S, Wittmer ST, Tucker-Heard G, Moon JJ, Jenkins MK, Urdahl KB, Winslow GM, Woodland DL. Distinct functions of antigen-specific CD4 T cells during murine Mycobacterium tuberculosis infection. Proc Natl Acad Sci USA. 2010; 107:19408–19413. [PubMed: 20962277]
12. Sarkar S, Kalia V, Haining WN, Konieczny BT, Subramaniam S, Ahmed R. Functional and genomic profiling of effector CD8 T cell subsets with distinct memory fates. J Exp Med. 2008; 205:625–640. [PubMed: 18316415]
13. Voehringer D, Blaser C, Brawand P, Raulet DH, Hanke T, Pircher H. Viral infections induce abundant numbers of senescent CD8 T cells. J Immunol. 2001; 167:4838–4843. [PubMed: 11673487]
14. Wiesel M, Crouse J, Bedenikovic G, Sutherland A, Joller N, Oxenius A. Type-I IFN drives the differentiation of short-lived effector CD8+ T cells in vivo. Eur J Immunol. 2012; 42:320–329. [PubMed: 22102057]
15. Jung YW, Rutishauser RL, Joshi NS, Haberman AM, Kaech SM. Differential localization of effector and memory CD8 T cell subsets in lymphoid organs during acute viral infection. J Immunol. 2010; 185:5315–5325. [PubMed: 20921525]
16. Grundemann C, Schwartzkopff S, Koschella M, Schweier O, Peters C, Voehringer D, Pircher H. The NK receptor KLRG1 is dispensable for virus-induced NK and CD8+ T-cell differentiation and function in vivo. Eur J Immunol. 2010; 40:1303–1314. [PubMed: 20201037]
17. Prlic M, Sacks JA, Bevan MJ. Dissociating markers of senescence and protective ability in memory T cells. PLoS ONE. 2012; 7:e32576. [PubMed: 22396780]
18. Beyersdorf N, Ding X, Tietze JK, Hanke T. Characterization of mouse CD4 T cell subsets defined by expression of KLRG1. Eur J Immunol. 2007; 37:3445–3454. [PubMed: 18034419]
19. Stephens GL, Andersson J, Shevach EM. Distinct subsets of FoxP3+ regulatory T cells participate in the control of immune responses. J Immunol. 2007; 178:6901–6911. [PubMed: 17513739]
20. Rosenblum MD, Gratz IK, Paw JS, Lee K, Marshak-Rothstein A, Abbas AK. Response to self antigen imprints regulatory memory in tissues. Nature. 2011; 480:538–542. [PubMed: 22121024]
21. Layland LE, Mages J, Loddenkemper C, Hoerauf A, Wagner H, Lang R, da Costa CU. Pronounced phenotype in activated regulatory T cells during a chronic helminth infection. J Immunol. 2010; 184:713–724. [PubMed: 20007528]
22. Feuerer M, Hill JA, Kretschmer K, von BH, Mathis D, Benoist C. Genomic definition of multiple ex vivo regulatory T cell subphenotypes. Proc Natl Acad Sci US A. 2010; 107:5919–5924.

23. Chauhan SK, Saban DR, Lee HK, Dana R. Levels of Foxp3 in regulatory T cells reflect their functional status in transplantation. J Immunol. 2009; 182:148–153. [PubMed: 19109145]
24. Kuczma M, Pawlikowska I, Kopij M, Podolsky R, Rempala GA, Kraj P. TCR repertoire and Foxp3 expression define functionally distinct subsets of CD4+ regulatory T cells. J Immunol. 2009; 183:3118–3129. [PubMed: 19648277]
25. Coleman MM, Finlay CM, Moran B, Keane J, Dunne PJ, Mills KH. The immunoregulatory role of CD4(+) FoxP3(+) CD25(−) regulatory T cells in lungs of mice infected with Bordetella pertussis. FEMS Immunol Med Microbiol. 2012; 64:413–424. [PubMed: 22211712]
26. Nishioka T, Shimizu J, Iida R, Yamazaki S, Sakaguchi S. CD4+CD25+Foxp3+ T cells and CD4+CD25−Foxp3+ T cells in aged mice. J Immunol. 2006; 176:6586–6593. [PubMed: 16709816]
27. Bonelli M, Savitskaya A, Steiner CW, Rath E, Smolen JS, Scheinecker C. Phenotypic and functional analysis of CD4+ J Immunol. 2009; 182:1689–1695. [PubMed: 19155519]
28. Huan J, Culbertson N, Spencer L, Bartholomew R, Burrows GG, Chou YK, Bourdette D, Ziegler SF, Offner H, Vandenbark AA. Decreased FOXP3 levels in multiple sclerosis patients. J Neurosci Res. 2005; 81:45–52. [PubMed: 15952173]
29. Zabransky DJ, Nirschl CJ, Durham NM, Park BV, Ceccato CM, Bruno TC, Tam AJ, Getnet D, Drake CG. Phenotypic and functional properties of Helios+ regulatory T cells. PLoS ONE. 2012; 7:e34547. [PubMed: 22479644]
30. Akimova T, Beier UH, Wang L, Levine MH, Hancock WW. Helios expression is a marker of T cell activation and proliferation. PLoS ONE. 2011; 6:e24226. [PubMed: 21918685]
31. Nguyen P, Liu W, Ma J, Manirarora JN, Liu X, Cheng C, Geiger TL. Discrete TCR repertoires and CDR3 features distinguish effector and Foxp3+ regulatory T lymphocytes in myelin oligodendrocyte glycoprotein-induced experimental allergic encephalomyelitis. J Immunol. 2010; 185:3895–3904. [PubMed: 20810983]
32. Liu X, Nguyen P, Liu W, Cheng C, Steeves M, Obenauer JC, Ma J, Geiger TL. T cell receptor CDR3 sequence but not recognition characteristics distinguish autoreactive effector and Foxp3(+) regulatory T cells. Immunity. 2009; 31:909–920. [PubMed: 20005134]
33. Selvaraj RK, Geiger TL. A kinetic and dynamic analysis of Foxp3 induced in T cells by TGF-beta. J Immunol. 2007; 178:7667–7677. [PubMed: 17548603]
34. Floess S, Freyer J, Siewert C, Baron U, Olek S, Polansky J, Schlawe K, Chang HD, Bopp T, Schmitt E, Klein-Hessling S, Serfling E, Hamann A, Huehn J. Epigenetic control of the foxp3 locus in regulatory T cells. PLoS Biol. 2007; 5:e38. [PubMed: 17298177]
35. Mann MK, Maresz K, Shriver LP, Tan Y, Dittel BN. B cell regulation of CD4+CD25+ T regulatory cells and IL-10 via B7 is essential for recovery from experimental autoimmune encephalomyelitis. J Immunol. 2007; 178:3447–3456. [PubMed: 17339439]
36. Ferber IA, Brocke S, Taylor-Edwards C, Ridgway W, Dinisco C, Steinman L, Dalton D, Fathman CG. Mice with a disrupted IFN-gamma gene are susceptible to the induction of experimental autoimmune encephalomyelitis (EAE). J Immunol. 1996; 156:5–7. [PubMed: 8598493]
37. Chu CQ, Wittmer S, Dalton DK. Failure to suppress the expansion of the activated CD4 T cell population in interferon gamma-deficient mice leads to exacerbation of experimental autoimmune encephalomyelitis. J Exp Med. 2000; 192:123–128. [PubMed: 10880533]
38. McGeachy MJ, Stephens LA, Anderton SM. Natural recovery and protection from autoimmune encephalomyelitis: contribution of CD4+CD25+ regulatory cells within the central nervous system. J Immunol. 2005; 175:3025–3032. [PubMed: 16116190]
39. Gupta S, Thornley TB, Gao W, Larocca R, Turka LA, Kuchroo VK, Strom TB. Allograft rejection is restrained by short-lived TIM-3+PD-1+Foxp3+ Tregs. J Clin Invest. 2012; 122:2395–2404. [PubMed: 22684103]
40. Huang CT, Workman CJ, Flies D, Pan X, Marson AL, Zhou G, Hipkiss EL, Ravi S, Kowalski J, Levitsky HI, Powell JD, Pardoll DM, Drake CG, Vignali DA. Role of LAG-3 in regulatory T cells. Immunity. 2004; 21:503–513. [PubMed: 15485628]
41. Chang LY, Lin YC, Kang CW, Hsu CY, Chu YY, Huang CT, Day YJ, Chen TC, Yeh CT, Lin CY. The Indispensable Role of CCR5 for In Vivo Suppressor Function of Tumor-Derived CD103+ Effector/Memory Regulatory T Cells. J Immunol. 2012; 189:567–574. [PubMed: 22664873]

42. O'connor RA, Anderton SM. Foxp3+ regulatory T cells in the control of experimental CNS autoimmune disease. J Neuroimmunol. 2008; 193:1–11. [PubMed: 18077005]

43. Apostolou I, von BH. In vivo instruction of suppressor commitment in naive T cells. J Exp Med. 2004; 199:1401–1408. [PubMed: 15148338]

44. Weiner HL, da Cunha AP, Quintana F, Wu H. Oral tolerance. Immunol Rev. 2011; 241:241–259. [PubMed: 21488901]

45. Joshi NS, Cui W, Chandele A, Lee HK, Urso DR, Hagman J, Gapin L, Kaech SM. Inflammation directs memory precursor and short-lived effector CD8(+) T cell fates via the graded expression of T-bet transcription factor. Immunity. 2007; 27:281–295. [PubMed: 17723218]

46. Cheng G, Yuan X, Tsai MS, Podack ER, Yu A, Malek TR. IL-2 Receptor Signaling Is Essential for the Development of Klrg1+ Terminally Differentiated T Regulatory Cells. J Immunol. 2012

47. Ferber IA, Brocke S, Taylor-Edwards C, Ridgway W, Dinisco C, Steinman L, Dalton D, Fathman CG. Mice with a disrupted IFN-gamma gene are susceptible to the induction of experimental autoimmune encephalomyelitis (EAE). J Immunol. 1996; 156:5–7. [PubMed: 8598493]

48. Komiyama Y, Nakae S, Matsuki T, Nambu A, Ishigame H, Kakuta S, Sudo K, Iwakura Y. IL-17 plays an important role in the development of experimental autoimmune encephalomyelitis. J Immunol. 2006; 177:566–573. [PubMed: 16785554]

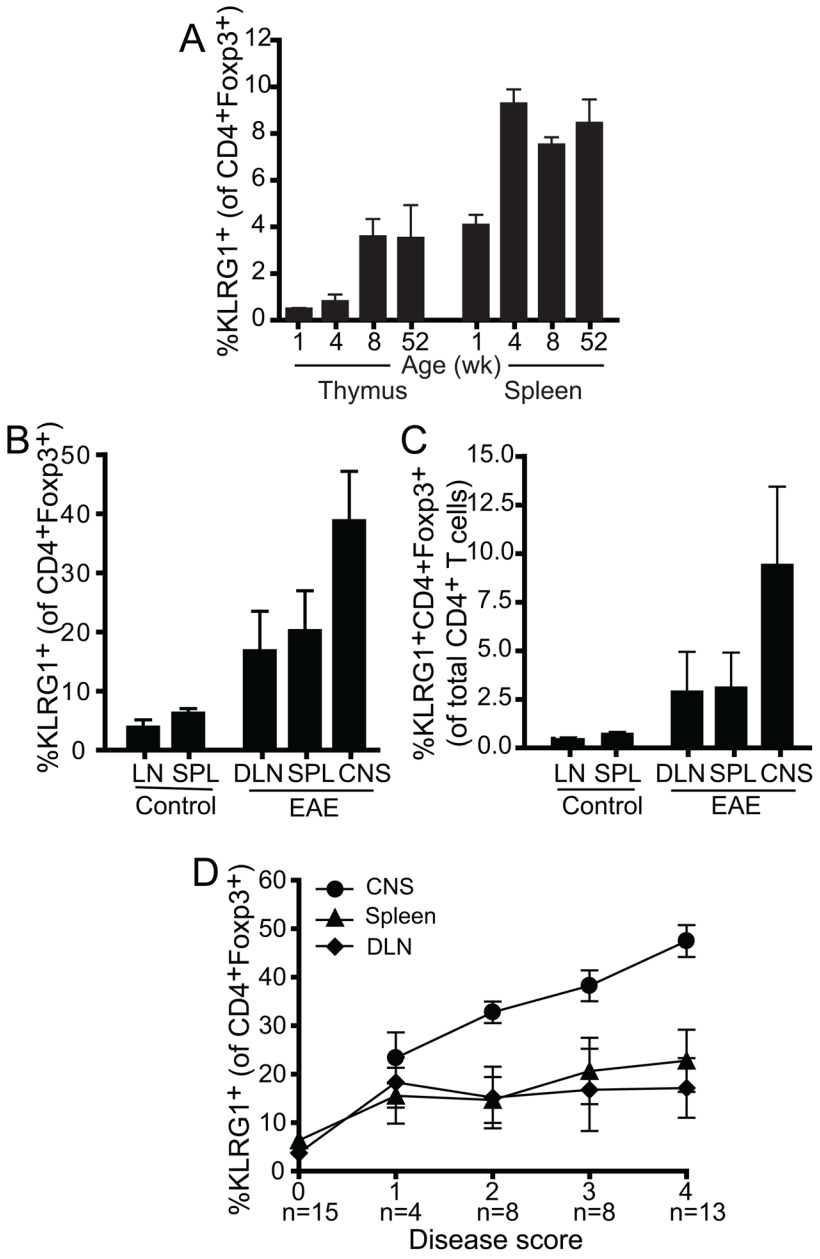

Figure 1. Increased Treg KLRG1 expression with EAE

(A) Cell surface expression of KLRG1 was examined on thymic and splenic Treg from 1, 4, 8 and 52 wk old mice. (B, C) Number of KLRG1$^+$ Treg was quantified at the indicated sites from mice with EAE (d 14) or unimmunized controls. Representative of five experiments with n= 5–7 per cohort. Data is plotted relative to total Treg (B) or total CD4$^+$ T cell numbers (C). (D) Percent CD4$^+$Foxp3$^+$KLRG1$^+$ cells is plotted versus disease score. Mice with a disease score of 0 are unimmunized, and with scores of 1 – 4 are d 14 post EAE induction. Number of mice with the indicated score is listed. Mean ± 1 s.d. is plotted.

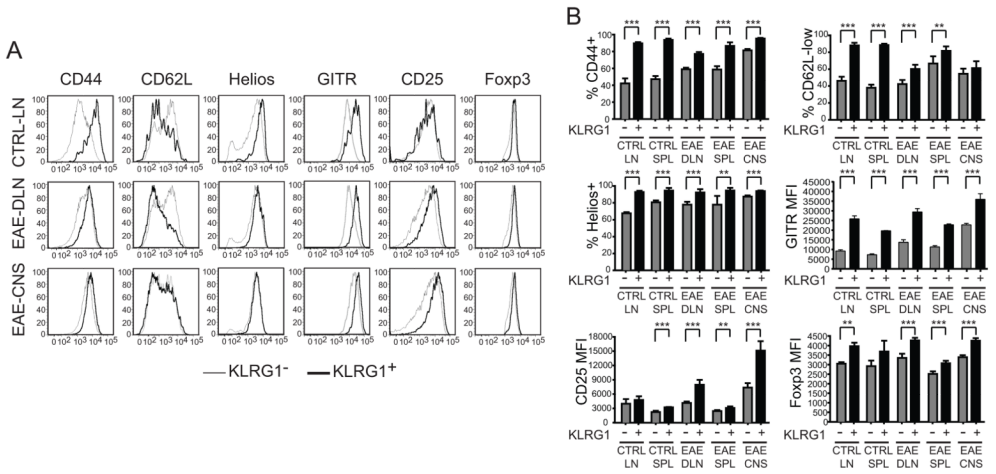

Figure 2. Activation status of KLRG1$^+$ and KLRG1$^-$ Treg

KLRG1$^+$ or KLRG1$^-$ CD4$^+$TCR$^+$Foxp3$^+$ cells from mice 14 d after EAE induction or unimmunized controls were analyzed for the expression of the indicated markers. (A) Sample overlay histogram plots of KLRG1$^+$ and KLRG1$^-$ Treg from LN or CNS are shown. (B) Results from LN, spleen, and CNS are plotted as percent positive or low/negative where positive and negative populations could be delineated, or as mean of fluorescence intensity (MFI) where expression intensities varied. Results plotted are from 3–7 mice per group from a representative experiment. Mean + 1 s.d. is shown. *p< 0.05, **p< 0.01, ***p< 0.001.

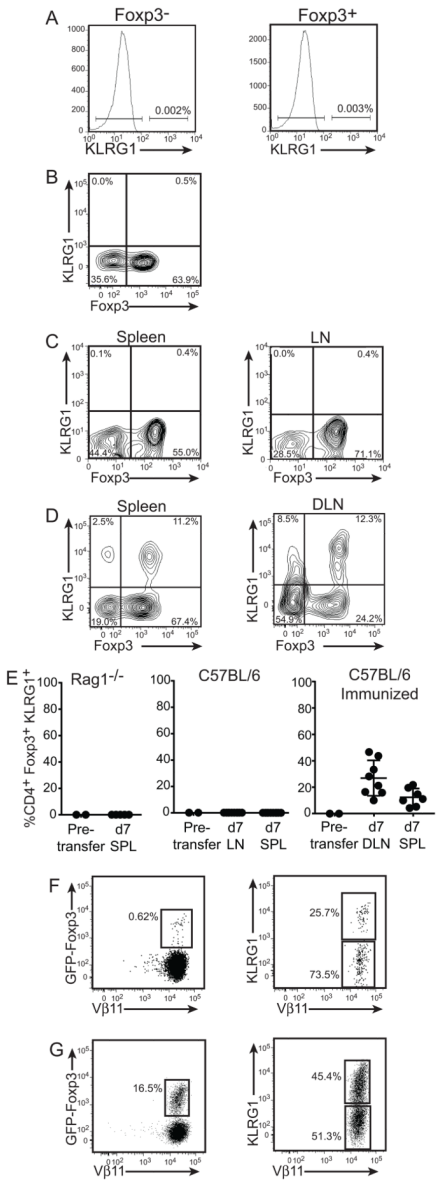

Figure 3. KLRG1 expression in iTreg

(A) iTreg were generated as described under Methods. Histogram plots show KLRG1 expression on gated Foxp3$^+$ or Foxp3$^-$ cells examined on d 5. Results are representative of 3 experiments. Flow cytometrically sorted CD45.1$^+$CD4$^+$GFP-Foxp3$^+$ iTreg (1×10^6) were then transferred into CD45.1$^-$CD45.2$^+$ Rag1$^{-/-}$ (B) or C57BL/6 (C) mice. Spleens (B) or spleens and LN (C) were harvested 7 d later and transferred iTreg analyzed for retention of Foxp3 and upregulation of KLRG1. iTreg gating is shown in Suppl. Fig. 2a. Data is representative of 2 experiments with 3 mice per cohort. In 2 additional experiments, EAE was induced in a subset of mice 1 d after iTreg transfer. KLRG1 upregulation was seen in the immunized mice (D) but, as in (C), not unimmunized controls (not shown). (E) The extent of KLRG1 upregulation among iTreg is plotted for 2 Rag1$^{-/-}$ transfer experiments (left) and 2 C57BL/6 transfers in which mice were unimmunized (middle) or EAE was induced (right). (F) EAE was next induced or allowed to spontaneously develop (G) in 2D2 TCR Tg/Rag1$^{-/-}$/GFP-Foxp3 mice. CNS-infiltrating T cells were isolated and

$CD4^+TCR(V\beta11)^+$ gated cells analyzed for Foxp3 upregulation (left plots). Expression of KLRG1 expression by the gated $Foxp3^+$ cells was assessed (right plots). Plots are representative of 6 mice and 2 experiments in (F) analyzed 15–25 d after EAE induction and 3 mice spontaneously developing EAE (age 7–17 wk) in (G). Mice were analyzed after reaching a disease score of 3–4.

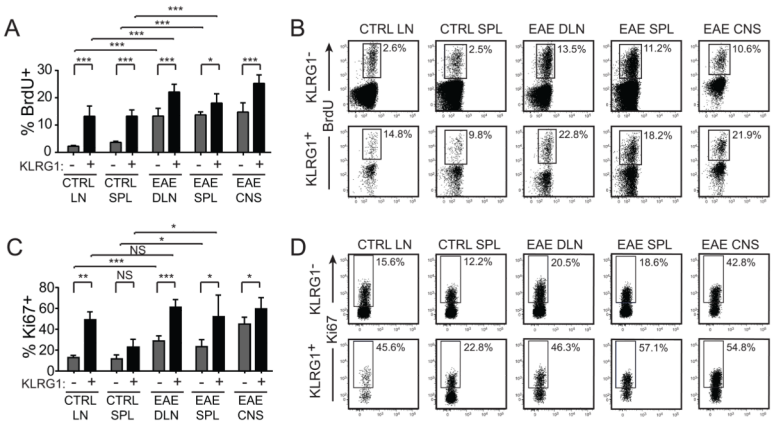

Figure 4. *In vivo* proliferation of KLRG1$^+$ and KLRG1$^-$ Treg

BrdU was administered to C57BL/6 mice that were unimmunized or had EAE (d 14). Sixteen h later, organs were harvested and cells stained for BrdU incorporation. (A) Percent BrdU$^+$ cells among the CD4$^+$Foxp3$^+$ KLRG1$^+$ or KLRG1$^-$ populations is plotted. (B) Sample flow cytometry plots of individual mice are shown. (C, D) Analysis of similarly gated populations from control mice or mice with EAE (d 14) for Ki67 expression. Results are from 3–7 mice per per cohort from representative analyses. Mean + 1 s.d. is shown. *p< 0.05, **p< 0.01, ***p< 0.001, NS, not significant.

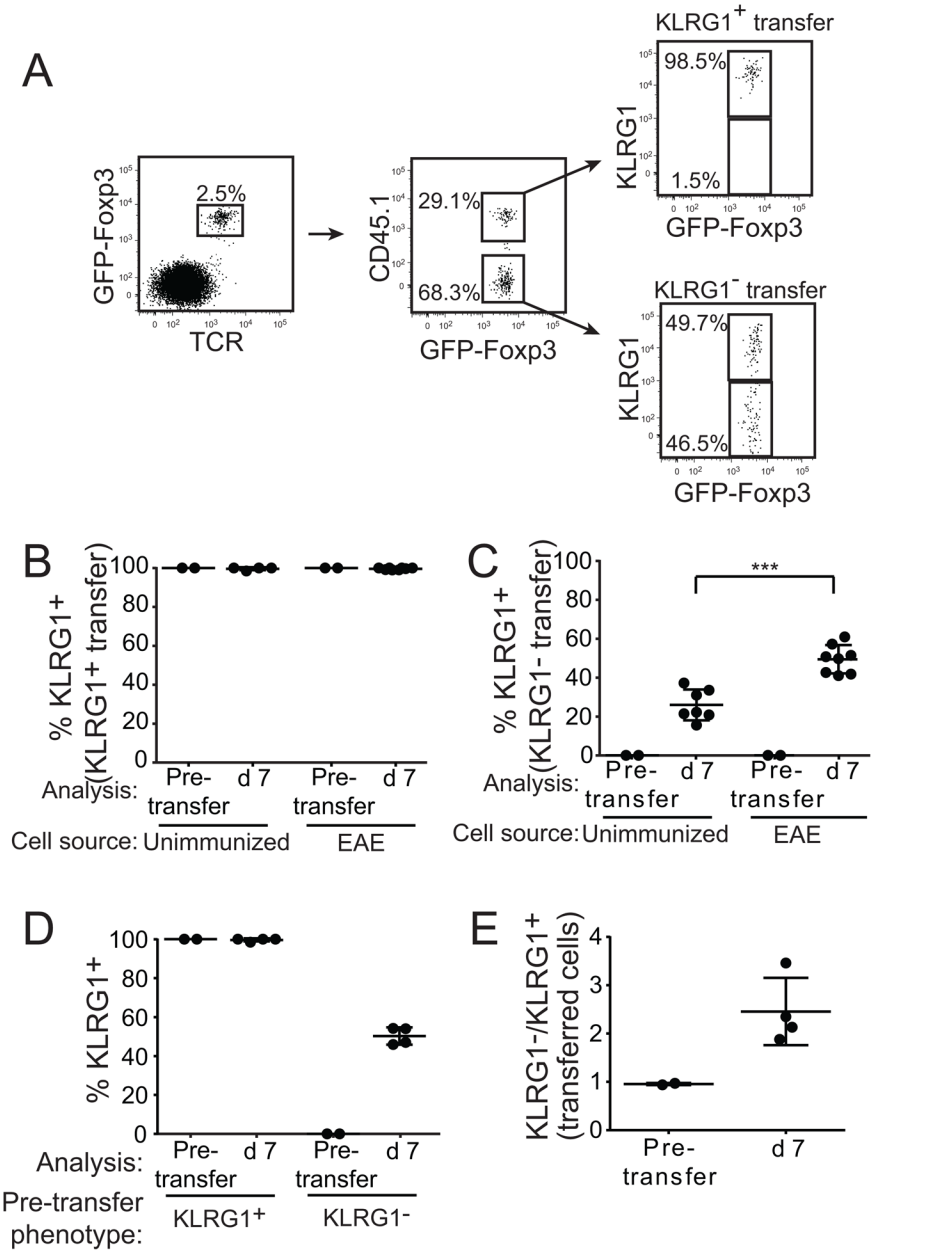

Figure 5. Unidirectional conversion of KLRG1$^-$ into KLRG1$^+$ Treg under lymphopenic conditions

Splenocytes from CD45.1 or CD45.2 mice with EAE (d 14) were sorted to obtain CD4$^+$GFP-Foxp3$^+$KLRG1$^+$ or CD4$^+$GFP-Foxp3$^+$KLRG1$^-$ populations. 5×10^5 congenic KLRG1$^+$ and KLRG1$^-$ cells were mixed at an ~1:1 ratio and adoptively co-transferred or transferred separately into Rag1$^{-/-}$ recipients. Mice were analyzed 7 d later. (A) Sample flow cytometry plots from an individual mouse receiving co-transferred KLRG1$^+$ and KLRG1$^-$ Treg demonstrate identification of transferred cells based on CD45 congenic marker expression. Additional gating information is provided in Suppl. Fig. 2b. (B, C) In 2 experiments, mice received separately transferred KLRG1$^+$ or KLRG1$^-$ Treg acquired from mice with EAE (d 14) or unimmunized controls. Percent of each transferred population (KLRG1$^+$ (B) or KLRG1$^-$ (C)) expressing KLRG1 immediately prior to or at d 7 after

transfer is plotted. (D, E) Data is plotted for 2 experiments in which congenic-marker distinguishable (CD45.1/CD45.2) KLRG1^{+} and KLRG1^{-} Treg from mice with EAE were mixed at a ~1:1 ratio prior to transfer and analyzed 7 d later. Expression of KLRG1 on each of the co-transferred populations (D) or the ratio of analyzed cells derived from transferred Treg populations that were originally KLRG1^{-} or KLRG1^{+} (E) is plotted. Mean±1 s.d. is shown.

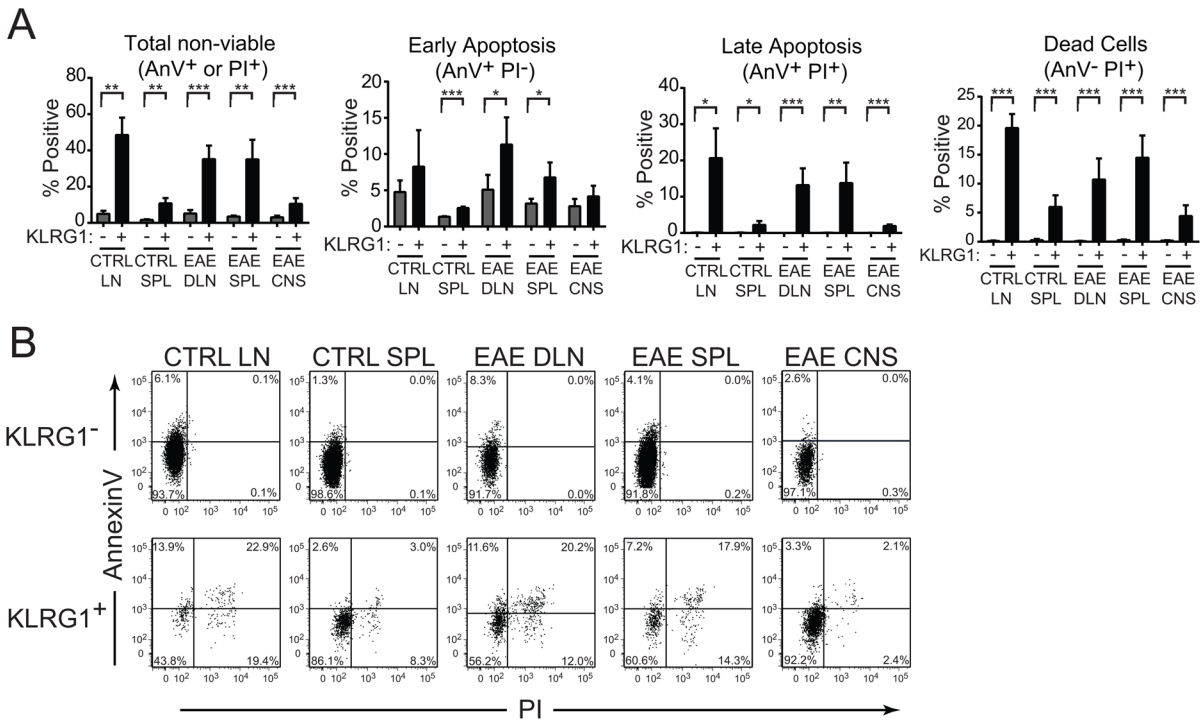

Figure 6. Annexin V and PI viability staining of KLRG1$^+$ and KLRG1$^-$ Treg

CD4$^+$TCR$^+$GFP-Foxp3$^+$ T lymphocytes from the indicated locations from mice with or without EAE (d 14) were gated into KLRG1$^+$ and KLRG1$^-$ populations, and assessed for AnnV and PI positivity. (A) Mean+1 s.d. is plotted for 1 of 2 similar experiments, each with 3–5 mice per experimental cohort, for total AnnV$^+$ or/and PI$^+$ cells, or subsets that were early or late apoptotic or dead. *, $p<0.05$, **, $p<0.01$, ***, $p<0.001$ in paired analyses. (B) Representative flow cytometry plots of gated KLRG1$^+$ or KLRG1$^-$ Treg from individual mice without (control) or with EAE demonstrate the enhanced death among the KLRG1$^+$ gated cells.

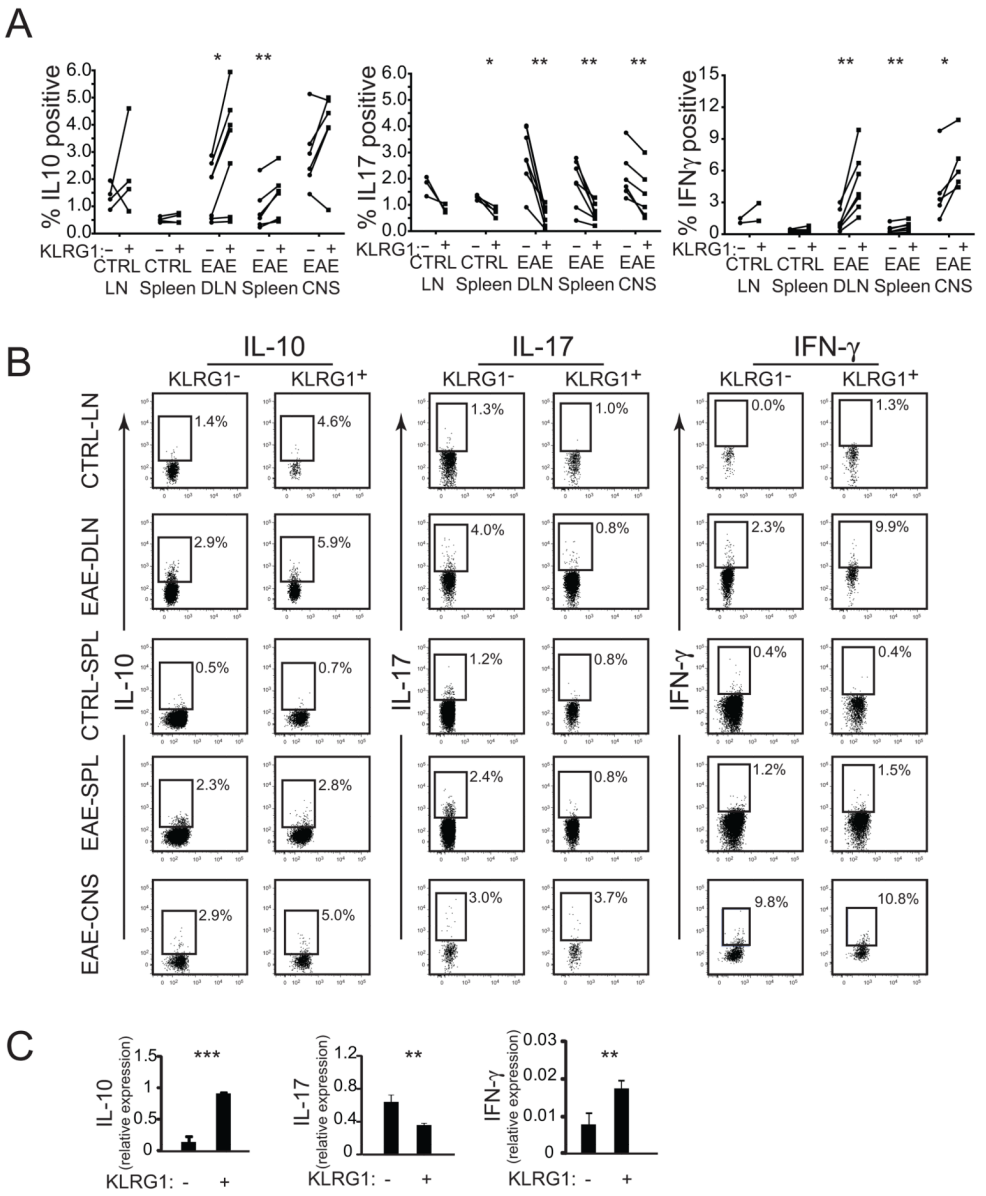

Figure 7. Cytokine profile of KLRG1$^+$ or KLRG1$^-$ Treg subsets

CNS, LN and splenic cells from unimmunized mice and mice with EAE (d 17) were briefly stimulated *ex vivo*, and stained by ICS for IL10, IL17 and IFNγ. (A) Percent of CD4$^+$TCR$^+$GFP-Foxp3$^+$ Treg positive for the indicated cytokine in different organs is plotted with lines connecting results for gated KLRG1$^+$ and KLRG1$^-$ cells from the same sample. Data are pooled from 2 experiments. (B) Representative flow cytometry plots are shown. Cytokine staining is plotted on the ordinate. The abscissa is a fluorescence channel unused for staining. (C) Quantitative RT-PCR analyzing relative expression of the above cytokines from splenic KLRG1$^+$ or KLRG1$^-$ Treg from mice with EAE flow sorted and stimulated as above is plotted. Data are representative of two experiments, with each sample analyzed in triplicate. Mean + 1 s.d. is plotted. *p< 0.05, **p< 0.01, ***, p<0.001.

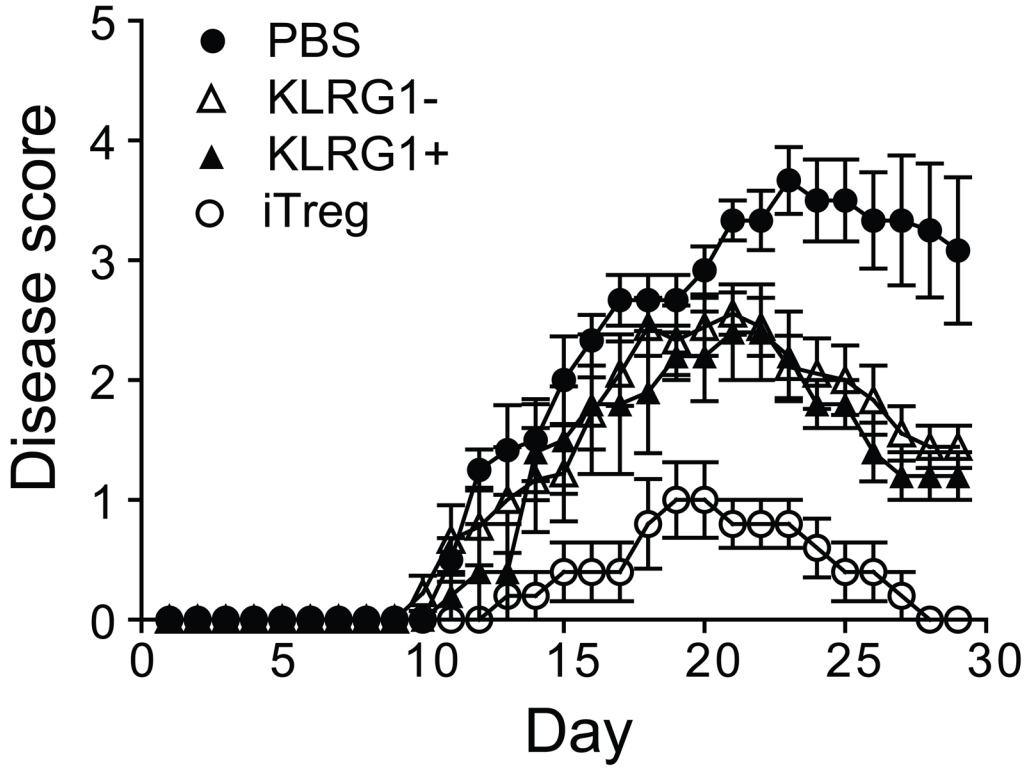

Figure 8. ***In vivo*** **suppression of EAE by KLRG1$^+$ or KLRG1$^-$ Treg subsets**

5×10^4 flow cytometrically purified CD4$^+$GFP-Foxp3$^+$KLRG1$^+$ or KLRG1$^-$ cells isolated from the CNS of mice with EAE (d 14), 10^6 iTreg, or saline was transferred into C57BL/6 mice one day prior to EAE induction. Clinical scores are plotted. The plot is a representative of 2 experiments with 5 – 9 mice per treatment group. Mean ± 1 s.e.m. is plotted.

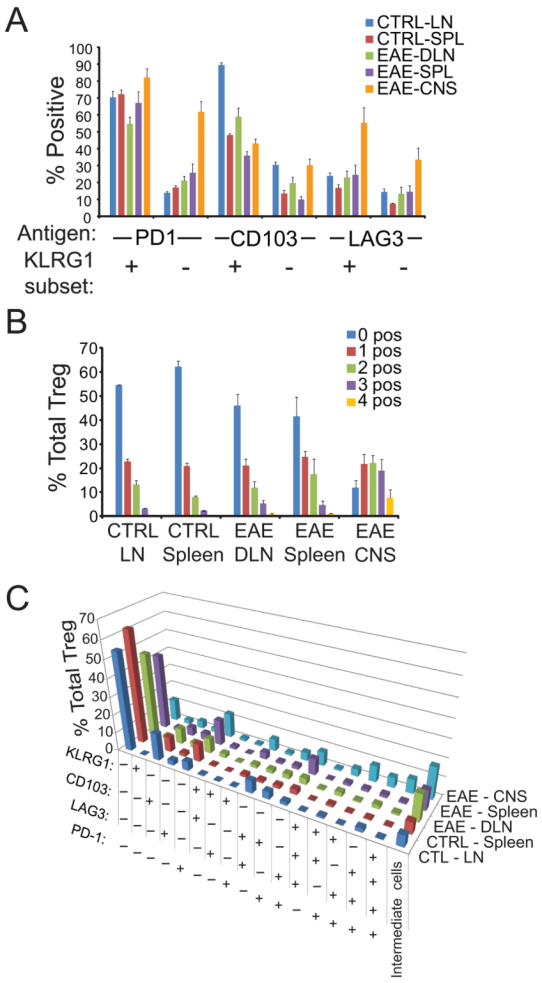

Figure 9. Phenotypic diversification of Foxp3$^+$ Treg during EAE

CNS, LN and splenic cells from unimmunized mice or mice with EAE (d 14) were isolated and Treg phenotype determined by analyzing CD4$^+$TCR$^+$Foxp3$^+$ gated cells for KLRG1, PD-1, CD103, and LAG3 expression. Gating and quantitation of cells expressing the individual markers is shown in Suppl. Fig. 5. (A) The percent of either KLRG1$^+$ or KLRG1$^-$ Treg that were also positive for the indicated second marker (PD-1, CD103, or LAG3) in each organ is plotted. Mean + 1 s.d. is shown. (D) The percent of total Tregs in the various organs that don't express any of the activation markers analyzed (0 pos), express a single marker (1 pos), 2 markers (2 pos), 3 markers (3 pos), or are positive for all markers (4 pos) is plotted. Mean + 1 s.d. is shown. (E) The percent of total Treg expressing the indicated marker pattern is plotted for each organ. Intermediate cells refers to cells that fell outside of the gates used to establish positive and negative expressing subsets, and so did not fall into any of the listed categories. Results are representative of 2 experiments with 4–6 mice per cohort.